2024 IEEE International Conference on Robotics and Automation (ICRA 2024)
May 13-17, 2024. Yokohama, Japan

DiPPeR: Diffusion-based 2D Path Planner applied on Legged Robots

Jianwei Liu*, Maria Stamatopoulou*, and Dimitrios Kanoulas

Abstract— **In this work, we present DiPPeR, a novel and fast 2D path planning framework for quadrupedal locomotion, leveraging diffusion-driven techniques. Our contributions include a scalable dataset generator for map images and corresponding trajectories, an image-conditioned diffusion planner for mobile robots, and a training/inference pipeline employing CNNs. We validate our approach in several mazes, as well as in real-world deployment scenarios on Boston Dynamic's Spot and Unitree's Go1 robots. DiPPeR performs on average 23 times faster for trajectory generation against both search based and data driven path planning algorithms with an average of 87% consistency in producing feasible paths of various length in maps of variable size, and obstacle structure. Website: https://rpl-cs-ucl.github.io/DiPPeR/**

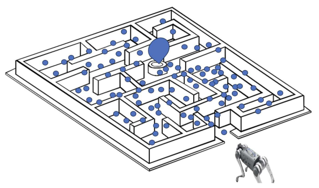
(a) Random Noise initialization

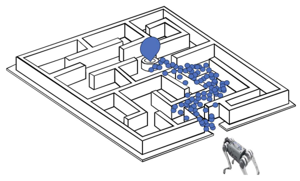
(b) Half way through denoising

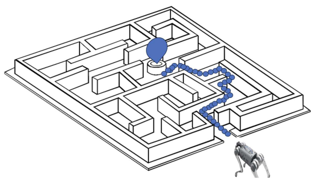
(c) Final denoised trajectory plan

Fig. 1: Illustration of DiPPeR global path generation process.

I. INTRODUCTION

Mobile robots, and especially legged ones, have the capacity to evolve into multi-purpose machines, useful in many application scenarios, such as production sites, household services, remote inspection, and disaster search-and-rescue [1]. Path planning is crucial in enabling legged robots to navigate autonomously and effectively complete the attributed tasks in various complex environments. Several studies, e.g., [2], [3], were dedicated towards the development of safe and efficient path planning algorithms, many of which utilize traditional methods such as Rapidly-exploring Random Trees (RRT) and A^*-based methods [4], [5]. However, such approaches often struggle to effectively handle the complexities and uncertainties associated with real-time sensor inputs [6]. Efficient and reliable path planning for quadrupeds is an ongoing challenge, with data driven approaches, such as Neural A* [7] and ViT-A* [8], showing promising efforts into overcoming the shortcomings of traditional approaches. Learning from demonstration methods using image conditioned Diffusion, have also shown promising results in path planning, applied mainly to manipulators [9], [10], [11], however, with minimal literature on their application on quadrupeds. Diffusion policies iteratively infer the action-score gradient, conditioned on visual observations. This allows for expression of multi-modal action distributions and scalability to higher-dimensional output space (allowing the generation of sequence of future actions), and training stability while maintaining distributional expressivity [9].

In this paper, we leverage the progress made in diffusion driven path planning, and develop an 2D path planning framework for quadrupedal locomotion. We develop a training and inference pipeline using a Convolutional Neural Network (CNN) based architecture. The main contributions of our method is the introduction of:

1) a scalable dataset comprising of randomly generated mazes and corresponding trajectories,
2) an image-conditioned diffusion planner for mobile robots,
3) trajectory generation significantly faster than both search based and data driven path planners and
4) a real-world deployment stack with a platform-invariant framework validation.

The remaining of the paper is structured as follows. In Sec. II, we briefly introduce literature in path planning relevant to our proposed method. In Sec. III, we provide the necessary background knowledge. In Sec. IV, we define our proposed method, with our experimental results presented in Sec. V. Finally, in Sec. VI, we summarize the results and we conclude with some future work.

The authors are with the RPL Lab, Department of Computer Science, University College London, Gower Street, WC1E 6BT, London, UK. {jianwei.liu.21, maria.stamatopoulou.21, d.kanoulas}@ucl.ac.uk

*equal contribution

This work was supported by the UKRI Future Leaders Fellowship [MR/V025333/1] (RoboHike) and the CDT for Foundational Artificial Intelligence [EP/S021566/1]. For the purpose of Open Access, the author has applied a CC BY public copyright license to any Author Accepted Manuscript version arising from this submission.

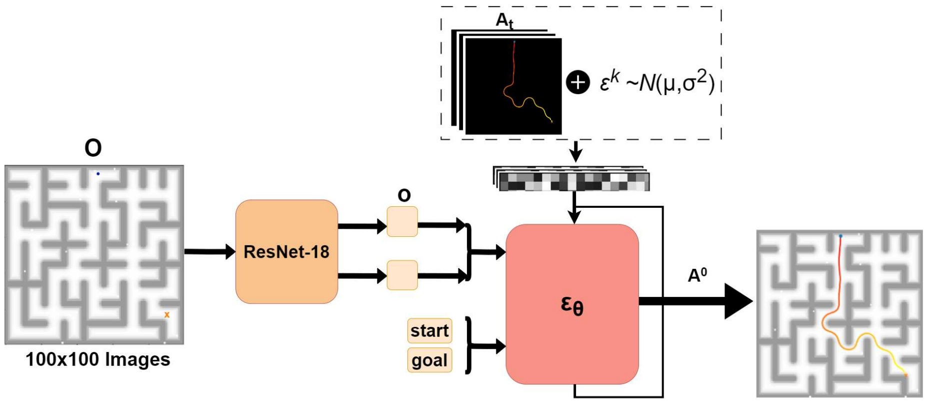

Fig. 2: DiPPeR - Image Conditioned Diffusion Training Pipeline: A Map Image Observations sample O is fed to the ResNet-18 Visual Encoder and converted to latent embeddings o. The x and y of the start and goal positions are also added as part of O. Noise ϵ^k sampled from the prior Gaussian Distribution is added to the trajectory instance A_t. The noisy sample is passed as an input to the diffusion network ϵ_θ and is conditioned by O. The network ϵ_θ takes the form of a CNN and it outputs the denoised action A^0.

II. RELATED WORK

Path planning algorithms, have a long history in robotics and are primarily split between classical and data-driven.

A. *Classical Path Planning*

Classical approaches in path planning rely on search-based and sampling-based methods. Search-based path planning provides mathematical guarantees of converging to a solution if it exists. A^* and its variations, offer simplicity in implementation and effectiveness to find valid paths. For instance, in very recent works [12], the authors introduced an extension of A^* to drive a mobile platform to sanitize rooms. In [13], an A^* algorithm was used to find the collision-free path for a legged robot to achieve autonomous navigation, while in [14], [15], similar path planners were developed for wheeled-legged path planning. For legged robots, the problem is connected to footstep planning too [16], [17], [18], where a sequence of footsteps are searched for navigation. Traditional methods heavily rely on fixed heuristic functions, such as the Euclidean distance, which lacks adaptability to varying robot configurations and environments and are usually computational heavy. In our work, such heuristics are not required as the path is learned through demonstration of multiple optimal trajectories.

Sampling-based planners efficiently create paths in high-dimensional spaces, by sampling points in the state space. Relevant literature in the field of quadrupedal robots include [2], where an extension of an RRT-based algorithm is used for controlling a quadruped robot during the DARPA Robotics Challenge in 2015. More recently in [3], a novel sampling-based planner was introduce to shorten the computational time for finding a new path for quadrupedal robots. While these approaches demonstrate satisfactory performance and probabilistic convergence, their limitations lie in the increasing planning time as the complexity of the environment increases, due to the iterative nature of the algorithms.

B. *Data-Driven Path Planning*

State-of-the-art research in the field has shifted towards incorporating machine learning techniques, which directly learn the behavior of path finding. These methods employ approaches such as expert demonstration [19] or imitation learning [6] to learn how to plan paths. Recent works directly address the issue of lack of semantically labeled maps in classical search-based methods by using data-driven approaches directly on raw image [20], [6], [21]. Specifically, Yonetani et al. [7] introduced Neural A^* (N-A^*) – a differentiable variant of the canonical A^*, coupled with a neural network trained end-to-end. The method works by encoding natural image inputs into guidance maps and searching for path-planning solutions on them, resulting in significant performance improvements over previous approaches in terms of efficiency. In an extension of N-A^*, Liu et al. [8] introduced ViT-A^*, that uses vision transformers for legged robot path planning which further improved the performance. However, as these method still relies on the A* to generate the final path, these methods would again results in increasing planning time as the complexity of the environment increases. Our proposed method, utilizes diffusion process to parallelize the generation of the entirety of the trajectory, overcoming this limitation.

C. *Diffusion for Path Planning*

Diffusion methods have gain popularity in the domain of path planing with many works presenting promising results. Hong et al. [22] developed diffusion maps applied to find a local path for reaching a goal and avoiding collisions with dynamic obstacles simultaneously, by computing transition probabilities between grid points. Janner et al. [11] and Chi et al. [9] developed impressive path planners, applied to robotic manipulators, by providing demonstration data and learning the trajectories through diffusion. We aim to leverage the promising results and develop a diffusion planing pipeline applied to quadrupedal locomotion.

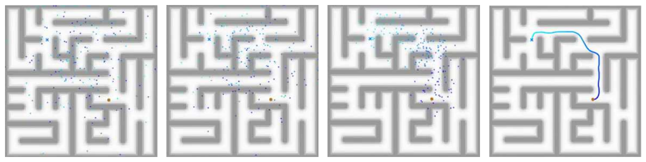
(a) $k = 0$ (b) $k = 300$ (c) $k = 700$ (d) $k = 1000$

Fig. 3: Denoising diffusion steps ($k = 1000$, $\text{path}_l = 200$) to generate a path from noisy samples.

III. Preliminaries

Path planning is essential for robot autonomous navigation and involves calculating a trajectory for a robot to follow in a map, between a start and end point. The solution of path planing refers to the generation of an optimal path, that full-fills the properties of finding the collision free, shortest, and smooth route between start and goal positions [23]. As elaborated in Sec. II, there are plethora of approaches to solve path planing. For relevance to our method we expand on Probabilistic Diffusion-based path planing, leveraging the learning capabilities of CNNs.

A. Diffusion

Image-guided diffusion models [24] have emerged as a powerful generative model with impressive performance when dealing with image datasets, among others. They provide the ability to transform a latent encoded representation into a more meaningful description of the image data. A popular variation is the Denoising Diffusion Probabilistic Model (DDPM), a generative model defined through parameterized Markov chains trained using variations inference. A forward chain converts input data into noise and a reverse chain converts the noisy data back to its original form. In particular, the noisy data $x^{1:N}$ is generated by iteratively adding Gaussian noise to the data x^0 according to a variance schedule $\beta^{1:N}$ [25]:

$$q(x^i \mid x^{i-1}) = \mathcal{N}(x^i; \sqrt{1-\beta^i}x^{i-1}, \beta^i \mathbf{I}) \tag{1}$$

Then, the denoising occurs by learning transition kernels parameterized using deep neural networks, for reversing the noisy data x^N back to the input x^0 [25], [26]. The learned denoising kernel $p_\theta(x^{i-1} \mid x^i)$ is parameterized by a prior Gaussian distribution starting at $p(x^N) = \mathcal{N}(x^N; \mathbf{0}, \mathbf{I})$ and is defined by:

$$p_\theta(x^{i-1} \mid x^i) = \mathcal{N}\left(x^{i-1}; \mu_\theta(x^i, i), \mathbf{\Sigma}_\theta(x^i, i)\right) \tag{2}$$

where, θ represents the model parameters, $\mu_\theta(x^i, i)$ the mean and $\mathbf{\Sigma}_\theta(x^i, i)$ the variance, parameterized by the deep neural network. A popular deep neural network choice for image conditioned diffusion are CNNs due to their benefits in dealing with image datasets.

IV. Method

Our method is inspired by the baseline papers [9], [11]. We adapt the image conditioned diffusion pipeline [9] to solve the problem of mobile robot path planing, while also conditioning for the starting and goal position of the trajectory via inpainting based on [11]. Initially the training dataset is generated, comprising of the 100x100 sized random and solvable maps and a number of trajectories for each map (Sec. IV-A). This is tenfold larger and more complicated dataset than the one provided in the baseline paper [11]. The dataset is fed into the training pipeline (Sec. IV-B), where the optimal trajectories are learned through demonstration by preserving local consistencies. The inference pipeline (Sec. V-A) allows the generation of the optimal trajectory given start and goal positions and the relevant map.

A. Data generation

Creating the training dataset includes generating random map images and feasible 2D trajectories. Examples of the randomly generated maps and trajectories are depicted in Fig. 4.

1) Map generation: Map generation is done through Kruskal's Minimum Spanning Tree (MST) Algorithm [27], with the edges representing potential wall locations and the nodes representing cells. The algorithm works by initially considering all edges of a randomly weighted graph and sorting them by their weights. Then, it iteratively adds edges to the MST, starting with the smallest weight, while ensuring that the graph remains acyclic. This process continues until all vertices are in the MST or the desired number of edges is reached. Kruskal's algorithm employs disjoint-set data structures to efficiently detect and avoid creating cycles during edge selection, resulting in a tree that spans all vertices with the minimum possible total edge weight.

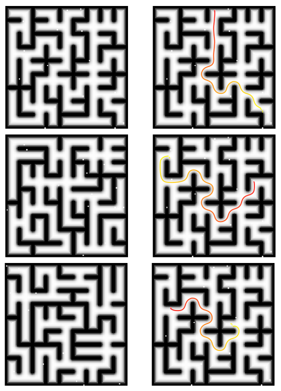
(a) Maps (b) Trajectories

Fig. 4: Generated samples from the dataset: 4a) examples of 100×100 random solvable maps and 4b) examples of trajectories, generated through A^*.

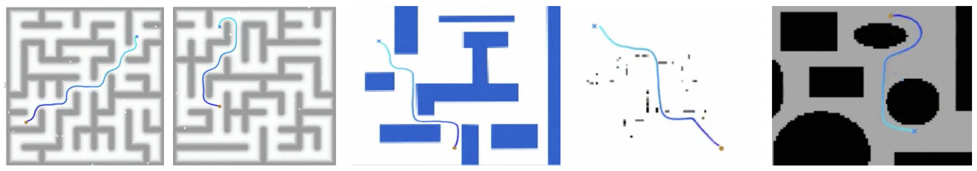

Fig. 5: Validating DiPPeR's performance and generalization. A random point is selected for the start and goal position on the provided map. Maps a) and b) are part of the validation dataset to validate the performance of the network in connecting the starting and end points while also avoiding the obstacles. Maps c),d) and e) are used to test the ability of the network to generalize to different out-of-distribution environments of varying scale, color and obstacle structure.

2) *Path generation:* To provide trajectories in the training framework, the generate paths need to be *feasible* - avoid all obstacles. To generate feasible paths we use the A^* path finding algorithm that uses a combination of heuristic estimates and cost information to efficiently find the shortest path between the start and end nodes. We randomize the position of the start and goal node to generate a variety of trajectories per map.

B. *Training Framework*

We formulate DiPPeR as a vision-guided mobile robot path planner generated through DDPMs, as presented in Sec. III. Our observation space O comprises of the 100×100 pixel images, representing the randomly generated maps. Our action space A_t comprises of 2D trajectories for each map. The subscript t refers to a sequence of timesteps, with $t = T$ representing the training horizon. We empirically conclude that a dataset of $10,000$ maps with 100 trajectories each, is sufficiently large to achieve generalization and adaptability to unseen maps. Fig. 2 provides a graphical representation of the proposed training framework.

DDPM Training: DDPM in our method, is used to approximate the conditional distribution $p(A_t \mid O)$ of the action vector A_t, given the map image observation O. This formulation speeds up the diffusion process and improves the generated actions by predicting an action conditioned to an observation, which translates to predicting trajectories given the specific map image.

DDPM takes as input A_t^k with added noise ϵ^k, sampled from the prior Gaussian distribution and performs k denoising iterations ($A_t^{k-1}, A_t^{k-2}, ..., A_t^0$) through gradient descent, following Eq. 3. The output is the noise free representation of the input vector A_t^0:

$$A_t^{k-1} = \alpha(A_t^k - \gamma\epsilon_\theta(O, A_t^k, k) + \mathcal{N}(0, \sigma^2 I)), \qquad (3)$$

where ϵ_θ represents the noise prediction network. The variables α, γ, σ and ϵ^k, when expressed as functions of k compose the noise schedule that drives the learning process, in this case, we've used the Square Cosine Schedule [28] in line with [9]. The hyperparameters α, γ, σ determine the scheduling learning rate which controls the extent to which the diffusion policy captures high and low-frequency characteristics of action signals.

Training ϵ_θ, involves predicting the noise added to a random sample A_t^0, through Eq. 3. For each A_t^0 a denoising iteration k is selected with an added corresponding noise value ϵ^k and variance. The mean squared error between the ϵ^k and the predicted noise value from ϵ_θ is then calculated based on Eq. 4, with the aim to be minimized along the gradient descent.

$$\mathcal{L} = MSE(\epsilon^k, \epsilon_\theta(O, A_t^0 + \epsilon^k, k)) \qquad (4)$$

By using inpainting-based goal state conditioning [11] and image conditioned diffusion [9], DiPPeR actions can be directly implemented to the real robot to find feasible trajectories connecting the start and goal positions given the map of the environment. We observe that varying the horizon length during training has a significant impact in the performance of the model. The generated trajectories in our dataset have variable length from 10 to 400, according to the A* generated path. The horizon length should be long enough to capture the whole range of the dataset, hence we set it equal to 180 which is the estimated average trajectory length.

An important design choice is selecting the architecture of ϵ_θ. We chose a CNN due to it being relative easy to tune compared to Transformers.

DiPPeR: We develop two variations of DiPPeR$_{cnn}$. The first version has observation space O as defined in Sec IV-B. The second version adds two extra terms to O, the trajectory start and end points, each expressed as a 2D vector corresponding to the x and y pixel coordinates. Whilst these extra start and goal conditions are not strictly necessary, as the inpainting-based start and goal conditioning are also used during inference, we have noticed that these extra conditions helped with convergance speed during training. A 1D temporal CNN is used with conditioning the actions generation on the observations by $p(A_t \mid O)$. The conditioning occurs through Feature-wise Linear Modulation (FiLM) [29] as proposed in [9].

Visual Encoder: A ResNet-18 visual encoder with spacial softmax pooling is trained end-to-end to convert the observation image O to a latent embedding o while preserving spatial information. The ResNet is trained alongside ϵ_θ.

V. RESULTS

A. *Inference Pipeline*

After training, the inference pipeline is used to validate DiPPeRs' performance. A start and goal position are randomly sampled from a uniform distribution and are then

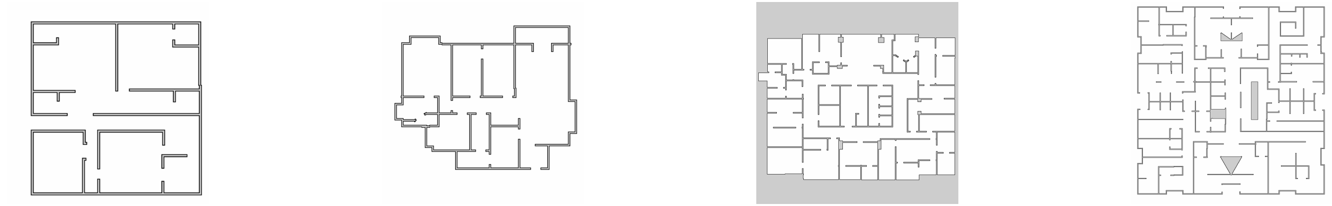

(a) office01
280 × 280

(b) room02
360 × 360

(c) office02
600 × 600

(d) mall
760 × 760

Fig. 6: MRPB benchmark dataset maps used for comparing different planning methods with their respective sizes.

passed into ϵ_θ, alongside O. A $path_l$ variable defines the number of noisy samples used during the denoising diffusion process. The value of path$_l$ is defined as function of the approximate length of the estimated trajectory, i.e. for start and goal positions being further apart, the $path_l$ will be larger and vice-versa. A vector of noise sampled from the prior Gaussian distribution with length equal to path$_l$ and 2 dimensions (x and y pixel coordinates) is constructed with the inpainting conditioning (i.e. the first and last column of the noise vector being set to the start and goal positions, respectively), is fed in the DiPPeR. The reverse chain of the DDPM model is used to iteratively denoise the input vector. The output is the final trajectory A_0, connecting the start and goal points, while aiming to follow a feasible path. The progress of denoising during inference is depicted in Fig. 3.

B. Simulation Results

The evaluation of DiPPeR's performance is completed in two stages. *Performance* evaluation is performed by sampling map images from the validation dataset and *Out-of-distribution* evaluation which is performed by selecting unseen map images of varying scale, color and obstacle structure to test DiPPeR's generalization capabilities. In both cases a random start and goal position is selected along the map and inference is performed following Sec. V-A. For all experiments the number of diffusion iterations is empirically chosen as $k = 1000$, to ensure both full convergence and minimum inference time. In most cases convergence is achieved with a smaller k however we decide to keep it constant to preserve uniformity across experiments. The path length path$_l$ parameter has a significant impact on the diffusion performance and needs to be varied according to the desired trajectory length. Given the start and goal position and the structure of the map, the number of feasible pixels can be measured to create an approximate estimation of path$_l$. Significantly larger path$_l$ will results in trajectories that loops locally and significantly smaller path$_l$ result in trajectories going through obstacles to connect the start and end goal. The chosen evaluation metric is the success rate. Success is achieved when the output trajectory A_0 connects the start and goal points while following a feasible path. Some examples of achieved successful trajectories are shown in Fig. 5. We evaluate DiPPeR in 10 images from the validation set and 10 out-of-distribution maps. For each map we generate 10 random start and goal positions and repeat inference 3 times, to ensure consistency of the output. The success rate is calculated by dividing the number of successful experiments by the total number experiments and is then converted to a percent value. The start and goal position conditioned version of the DiPPeR outperformed the non-conditioned one in all tests and we set it as our default DiPPeR version.

The percentage success rate $\%sr$ for DiPPeR is presented in Table I.

Dataset	$\%sr$
Validation	85
Out-of-Distribution	89
Average	87

TABLE I: Inference success rate for validation and out-of-distribution datasets.

DiPPeR is on average 87% successful in providing feasible paths. It performs best on out-of-distribution maps as they contain instances of maps much simpler in terms obstacle structure than the training dataset. To understand the failure cases, we plot the success rate against the trajectory length (Fig. 8). The success rate drops for both extremes of smaller and larger trajectories and performs the best for trajectories of length close to 180. This is expected as the choice of horizon length is set equal to 180 during training, however it presents a limitation that we aim to address in future work.

We consistent the same experiments in the real-word with the results being consistent with the simulation ones.

To assess the performance of DiPPeR against SOTA path planning frameworks, we evaluate its convergence speed against a search-based planner A^* and its data driven variants N-A^* [7] and ViT-A^* [8]. We compare the algorithms by using maps of increasing size and obstacle structure depicted on Fig. 6. For each map 10 trajectories with random start and end points are generated by the 4 algorithms. The time taken for trajectory generation is measured for all experiments and the 10 values for each map are averaged. The results are summarized in Table II.

The maps for comparison are sampled from the MRPB benchmark dataset [30].

All experiments were conducted using a NVIDIA RTX 3090 GPU. DiPPeR is on average 23 times faster against the next best performing SOTAs algorithms, with feasible trajectory generation taking only $0.4s$ regardless of maze size

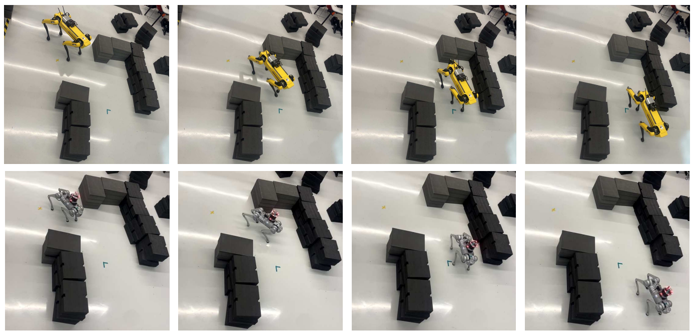

Fig. 7: Real World Deployment: Spot (top) and Go1 (bottom) navigating around a maze environment using DiPPER in combination with the developed navigation stack (Fig. 9).

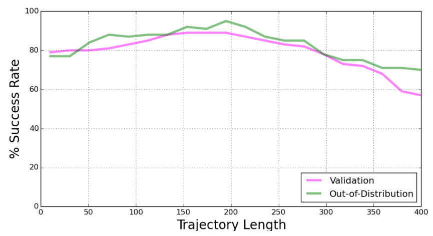

Fig. 8: Plot of the average % success rate against the trajectory length for maps sampled from the Validation and the Out-of-Distribution Dataset

maps	DiPPeR	ViT-A^*	N-A^*	A^*
(a)	**0.4**	5.68	4.70	6.03
(b)	**0.4**	17.31	14.73	17.51
(c)	**0.4**	4.81	5.17	15.59
(d)	**0.4**	12.73	16.57	36.24

TABLE II: Average time in seconds taken for trajectory generation by DiPPeR, ViT-A^*, N-A^*, A^*. Maps a)-d) are presented in Fig. 6.

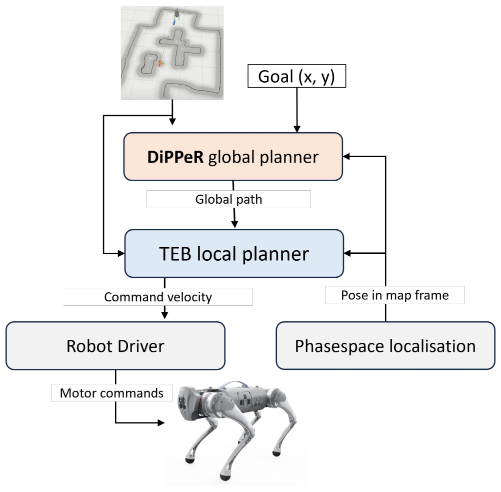

Fig. 9: Schematic structure of the navigation stack for DiPPeR real robot deployment.

or trajectory length. This is due to the generative properties of diffusion planner.

C. Real-World Deployment

A schematic representation of the real work deployment of DiPPeR is depicted in Fig. 9. We validate the performance of DiPPeR in the real world and its platform agnostic property through deployment on Unitree Go1[1] and Boston Dynamics Spot[2].

In order to leverage the existing robot navigation frameworks, DiPPeR is integrated with the 2D ROS navigation Stack[3], to act as a global path planner. Given the occupancy map, DiPPeR generates a global path which is further refined by the local planner – to avoid violation of the robots kinodyanmics constraints and an external tracking system – to mitigate for state estimation inaccuracies. The local planner used is the Timed-Elastic-Band (TEB) [31], [32] and the external tracker of choice is Phasespace tracking cameras[4]. Phasespace cameras allow for 960 Hz robot real-time localization. Examples of successful deployment of the pipeline can be seen in Fig. 7.

[1]https://www.unitree.com/en/go1/
[2]https://www.bostondynamics.com/products/spot
[3]http://wiki.ros.org/navigation

VI. CONCLUSION

In this paper we present DiPPeR, an image guided diffusion based 2D-path planner. The planner is successful in generating feasible paths of variable length on average 80% of the time, for maps of various size and obstacle structure. DiPPeR outperformed in speed against both search based and data driven planner by a factor of 23. We validate the transfer of the planner in the real world and showcase its platform agnostic capabilities by successfully testing it on two different robots. We identified that DiPPeR tends to performs less optimally for trajectories significantly longer than the training horizon, as well as requiring an estimate of the number of step for the final trajectory during inference. We are aiming to address this in future work by also experimenting with different network architectures, such as transformers, that show promising results in the field of diffusion.

[4]https://www.phasespace.com/

References

[1] N. Kottege, L. Sentis, and D. Kanoulas, "Editorial: Towards real-world deployment of legged robots," *Frontiers in Robotics and AI*, vol. 8, 2022.

[2] C. Lau and K. Byl, "Smooth RRT-Connect: An Extension of RRT-connect for Practical Use in Robots," in *IEEE International Conference on Technologies for Practical Robot Applications*, 2015, pp. 1–7.

[3] Y. Zhang, H. Jiang, X. Zhong, X. Zhong, and J. Zhao, "MI-RRT-Connect Algorithm for Quadruped Robotics Navigation with Efficiently Path Planning," *Journal of Physics: Conference Series*, vol. 2402, no. 1, 2022.

[4] D. Kanoulas, N. G. Tsagarakis, and M. Vona, "Curved Patch Mapping and Tracking for Irregular Terrain Modeling: Application to Bipedal Robot Foot Placement," *Robotics and Autonomous Systems*, vol. 119, pp. 13–30, 2019.

[5] V. Suryamurthy, V. S. Raghavan, A. Laurenzi, N. G. Tsagarakis, and D. Kanoulas, "Terrain Segmentation and Roughness Estimation using RGB Data: Path Planning Application on the CENTAURO Robot," in *IEEE-RAS 19th International Conference on Humanoid Robots (Humanoids)*, 2019, pp. 1–8.

[6] S. Choudhury, M. Bhardwaj, S. Arora, A. Kapoor, G. Ranade, S. Scherer, and D. Dey, "Data-Driven Planning via Imitation Learning," *The International Journal of Robotics Research*, vol. 37, no. 13-14, pp. 1632–1672, 2018.

[7] R. Yonetani, T. Taniai, M. Barekatain, M. Nishimura, and A. Kanezaki, "Path Planning Using Neural A* Search," in *International Conference on Machine Learning*, 2021, pp. 12 029–12 039.

[8] J. Liu, S. Lyu, D. Hadjivelichkov, V. Modugno, and D. Kanoulas, "ViT-A*: Legged Robot Path Planning using Vision Transformer A," in *IEEE-RAS 22nd International Conference on Humanoid Robots (Humanoids)*, 2023, pp. 1–6.

[9] C. Chi, S. Feng, Y. Du, Z. Xu, E. Cousineau, B. Burchfiel, and S. Song, "Diffusion Policy: Visuomotor Policy Learning via Action Diffusion," in *Robotics: Science and Systems (RSS)*, 2023.

[10] J. Carvalho, A. T. Le, M. Baierl, D. Koert, and J. Peters, "Motion planning diffusion: Learning and planning of robot motions with diffusion models," in *2023 IEEE/RSJ International Conference on Intelligent Robots and Systems (IROS)*. IEEE, 2023, pp. 1916–1923.

[11] M. Janner, Y. Du, J. Tenenbaum, and S. Levine, "Planning with Diffusion for Flexible Behavior Synthesis," in *International Conference on Machine Learning*, 2022.

[12] H. Huang, Y. Li, and Q. Bai, "An improved A* Algorithm for Wheeled Robots Path Planning with Jump Points Search and Pruning Method," *Complex Eng Syst*, vol. 2, p. 11, 2022.

[13] M. Kusuma, C. Machbub, *et al.*, "Humanoid Robot Path Planning and Rerouting Using A-Star Search Algorithm," in *2019 IEEE International Conference on Signals and Systems (ICSigSys)*, 2019, pp. 110–115.

[14] V. Sushrutha Raghavan, D. Kanoulas, D. G. Caldwell, and G. T. Nikos, "Reconfigurable and Agile Legged-Wheeled Robot Navigation in Cluttered Environments with Movable Obstacles," *IEEE Access*, 2021.

[15] K. Ellis, H. Zhang, D. Stoyanov, and D. Kanoulas, "Navigation Among Movable Obstacles with Object Localization using Photorealistic Simulation," in *IEEE/RSJ International Conference on Intelligent Robots and Systems (IROS)*, 2022, pp. 1711–1716.

[16] D. Kanoulas, C. Zhou, A. Nguyen, G. Kanoulas, D. G. Caldwell, and N. G. Tsagarakis, "Vision-Based Foothold Contact Reasoning using Curved Surface Patches," in *IEEE-RAS International Conference on Humanoids Robots (Humanoids)*, 2017, pp. 121–128.

[17] D. Kanoulas, A. Stumpf, V. Sushrutha Raghavan, C. Zhou, A. Toumpa, O. von Stryk, D. Caldwell, and N. Tsagarakis, "Footstep Planning in Rough Terrain for Bipedal Robots using Curved Contact Patches," in *IEEE Int. Conference on Robotics and Automation (ICRA)*, 2018.

[18] D. Kanoulas, N. G. Tsagarakis, and M. Vona, "Curved Patch Mapping and Tracking for Irregular Terrain Modeling: Application to Bipedal Robot Foot Placement," *Robotics and Autonomous Systems*, 2019.

[19] M. Pfeiffer, M. Schaeuble, J. Nieto, R. Siegwart, and C. Cadena, "From Perception to Decision: A Data-Driven Approach to End-to-End Motion Planning for Autonomous Ground Robots," in *IEEE International Conference on Robotics and Automation (ICRA)*, 2017, pp. 1527–1533.

[20] B. Ichter and M. Pavone, "Robot Motion Planning in Learned Latent Spaces," *IEEE Robotics and Automation Letters*, vol. 4, no. 3, pp. 2407–2414, 2019.

[21] L. Lee, E. Parisotto, D. S. Chaplot, E. Xing, and R. Salakhutdinov, "Gated Path Planning Networks," in *International Conference on Machine Learning*, 2018, pp. 2947–2955.

[22] S. Hong, J. Lu, and D. P. Filev, "Dynamic Diffusion Maps-based Path Planning for Real-time Collision Avoidance of Mobile Robots," in *IEEE Intelligent Vehicles Symposium (IV)*, 2018, pp. 2224–2229.

[23] S. G. Tzafestas, "Mobile Robot Path, Motion, and Task Planning," in *Introduction to Mobile Robot Control*. Elsevier, 2014, pp. 429–478.

[24] H. Ali, S. Murad, and Z. Shah, "Spot the Fake Lungs: Generating Synthetic Medical Images Using Neural Diffusion Models," in *Artificial Intelligence and Cognitive Science*, L. Longo and R. O'Reilly, Eds. Cham: Springer Nature Switzerland, 2023, pp. 32–39.

[25] J. Ho, A. Jain, and P. Abbeel, "Denoising diffusion probabilistic models," *Advances in neural information processing systems*, vol. 33, pp. 6840–6851, 2020.

[26] L. Yang, Z. Zhang, Y. Song, S. Hong, R. Xu, Y. Zhao, W. Zhang, B. Cui, and M.-H. Yang, "Diffusion Models: A Comprehensive Survey of Methods and Applications," *ACM Comput. Surv.*, 2023.

[27] J. B. Kruskal, "On the Shortest Spanning Subtree of a Graph and the Traveling Salesman Problem," *Proceedings of the American Mathematical society*, vol. 7, no. 1, pp. 48–50, 1956.

[28] A. Q. Nichol and P. Dhariwal, "Improved denoising diffusion probabilistic models," in *International Conference on Machine Learning*. PMLR, 2021, pp. 8162–8171.

[29] E. Perez, F. Strub, H. De Vries, V. Dumoulin, and A. Courville, "Film: Visual reasoning with a general conditioning layer," in *Proceedings of the AAAI conference on artificial intelligence*, vol. 32, no. 1, 2018.

[30] J. Wen, X. Zhang, Q. Bi, Z. Pan, Y. Feng, J. Yuan, and Y. Fang, "MRPB 1.0: A Unified Benchmark for the Evaluation of Mobile Robot Local Planning Approaches," in *IEEE International Conference on Robotics and Automation (ICRA)*, 2021, pp. 8238–8244.

[31] C. Rösmann, W. Feiten, T. Wösch, F. Hoffmann, and T. Bertram, "Trajectory Modification Considering Dynamic Constraints of Autonomous Robots," in *German Conference on Robotics (ROBOTIK)*. VDE, 2012, pp. 1–6.

[32] ——, "Efficient Trajectory Optimization Using a Sparse Model," in *European Conference on Mobile Robots*, 2013, pp. 138–143.